

# Solid state effects on exciton states and optical properties of PPV

Alice Ruini,<sup>1,2</sup> Marilia J. Caldas,<sup>3,1</sup> Giovanni Bussi,<sup>1,2</sup> and Elisa Molinari<sup>1,2</sup>

<sup>1</sup>*Istituto Nazionale per la Fisica della Materia (INFM)*

<sup>2</sup>*Dipartimento di Fisica, Università di Modena e Reggio Emilia, Via Campi 213a, I-41100 Modena, Italy*

<sup>3</sup>*Instituto de Fisica, Universidade de Sao Paulo, CP 66318, 05315-970 Sao Paulo, Brazil*

(Dated: October 28, 2018)

We perform *ab initio* calculations of optical properties for a typical semiconductor conjugated polymer, poly-*para*-phenylenevinylene, in both isolated chain and crystalline packing. In order to obtain results for excitonic energies and real-space wavefunctions we explicitly include electron-hole interaction within the density-matrix formalism. We find that the details of crystalline arrangement crucially affect the optical properties, leading to a richer exciton structure and opening non-radiative decay channels. This has implications for the optical activity and optoelectronic applications of polymer films.

PACS numbers: 71.15.Qe, 71.20.Rv, 71.35.-y

Ordered films of organic conjugated polymers are of strategic relevance for novel optoelectronic devices [1]. In addition, they offer an ideal scenario for the study of electronic and excitonic confinement, being composed of quasi-one-dimensional (1D) systems, arranged however in a three-dimensional (3D) crystalline environment. Long linear chains can indeed be thought of as 1D systems with the highest degree of 1D confinement for a polyatomic system ( $\sim 2\text{-}5 \text{ \AA}$ ). Since the main optoelectronic characteristics derive from the mobile  $\pi$ -electrons, delocalized along the chain backbone, and non bonding to neighbouring chains, the vast majority of studies adopt the single-chain model: in fact, complete *ab initio* theoretical studies of the optical properties have been performed for isolated chains, highlighting the strong confinement expected for such systems [2, 3]. Recently, very simplified models of polymers in a “crystalline medium” have been approached through *ab initio* theory [4]; however the effect of crystal structure or side chains is completely neglected. This is also usual practice in the interpretation of experimental data: e.g. data on poly-*para*-phenylenevinylene (PPV) and its alkylated and methoxylated derivatives (MH-PPV, MEH-PPV, etc. . .) are usually bundled together as representative of PPV, based on the supposition that details of the 3D structure are not relevant. The picture emerging from this analysis is far from clear, however: quoted exciton binding energies differ by an order of magnitude [5, 6, 7, 8, 9, 10], there is an on-going controversy about the existence of charge-transfer excitons or excimers [8, 11, 12, 13, 14], and about conditions for efficient light emission. The question then arises if, on the contrary, solid state effects cannot be neglected and crystallization entails also structure-specific 3D interchain coupling effects: recent data on oligothiophene crystals seem to suggest that this might be the case [15, 16].

Here we address these issues through a full *ab initio* calculation of optical spectra and real-space exciton wavefunctions for PPV, in both the isolated chain and the

crystalline phase. In the single PPV chain, we find that the lowest singlet exciton extends over a few monomers along the chain and is optically active, with a binding energy of about  $0.6\div 0.7$  eV. In the crystal we find evidence of significant interchain coupling, with decrease of the first optically active exciton binding energy to about  $0.2\div 0.3$  eV [7, 8, 9]; as a consequence of both interchain interaction and detailed crystalline structure, a dark split-off singlet exciton appears at lower energy, which introduces a new path for non-radiative emission and electron-hole dissociation, and is expected to decrease drastically the photoluminescence efficiency [13]; furthermore, we find a much richer exciton structure, with charge-transfer excitons close enough to the first direct exciton [8] to account for early electron-hole dissociation and apparently-vanishing binding energies [10]; fitting all the pieces together, our results can explain the controversies on the optical behavior of these crystals.

The exciton binding energy,  $E_b$ , is a central quantity in the photophysics of polymer semiconductors because it is related to the spatial extension of the excitation and to the probability of radiative emission/absorption and electric-field-induced dissociation of the exciton. It is defined as the energy required to separate a bound electron-hole pair, the exciton, into a free electron and a free hole [7, 8, 9, 11, 17]. For PPV, the experimental values that are currently reported range from  $0.2\div 0.4$  eV [7, 8, 9] to around 1 eV [5, 6], but energies of less than 0.1 eV are also proposed [10]. These values correspond to spatial extensions varying from a single monomer (Frenkel-like excitons) up to many unit cells (Wannier-like excitons).

From the theoretical point of view, calculating the properties of excitons in extended polymeric systems is much more difficult than in conventional inorganic-semiconductor quantum wires [18], because it requires to combine an accurate treatment of the Coulomb interaction with a realistic microscopic description of the single-particle electronic structure beyond effective mass approximations. Standard quantum-chemistry schemes

[19] for treating excitations in finite molecular systems are intrinsically not suitable for crystals. To this end, we have implemented a first-principles density-matrix approach where the correlated electron-hole spectrum is obtained directly from the interband polarizations  $\langle d_\nu^\dagger c_\mu^\dagger \rangle$ , resulting from the creation of an electron in conduction state  $\mu$ , with energy  $\epsilon_\mu^e$  and a hole in valence state  $\nu$  with energy  $\epsilon_\nu^h$  ( $c_\mu^\dagger$  and  $d_\nu^\dagger$  are the Fermionic creation operators; the labels  $\mu = (c, \mathbf{k})$  and  $\nu = (v, \mathbf{k})$  stand for both the band index and the wavevector). The polarization eigenstates are obtained by direct diagonalization of the two-body Schrödinger equation:

$$(\bar{\epsilon}_\mu^e - \bar{\epsilon}_\nu^h) A_{\mu\nu} + e^2 \sum_{\mu'\nu'} (2\delta_S V_{\mu\nu',\nu\mu'} - W_{\mu\mu',\nu\nu'}) A_{\mu'\nu'} = E_x A_{\mu\nu}$$

Here the first term on the right-hand side accounts for the uncorrelated electron and hole quasi-particle energies, the second for electron-hole screened direct ( $W$ ) and unscreened exchange ( $V$ ) Coulomb interaction ( $\delta_S = 1$  for singlets, 0 otherwise). The interaction kernels are written in terms of the single-particle wavefunctions  $\psi$ :

$$W_{\mu\mu',\nu\nu'} = \int \psi_\mu^{e*}(\mathbf{r}_1) \psi_{\mu'}^e(\mathbf{r}_1) w(\mathbf{r}_1, \mathbf{r}_2) \psi_{\nu'}^{h*}(\mathbf{r}_2) \psi_\nu^h(\mathbf{r}_2) d\mathbf{r}_1 d\mathbf{r}_2$$

$$V_{\mu\nu',\nu\mu'} = \int \psi_\mu^{e*}(\mathbf{r}_1) \psi_{\nu'}^h(\mathbf{r}_1) v(\mathbf{r}_1, \mathbf{r}_2) \psi_\nu^{h*}(\mathbf{r}_2) \psi_{\mu'}^e(\mathbf{r}_2) d\mathbf{r}_1 d\mathbf{r}_2$$

where  $v(\mathbf{r}_1, \mathbf{r}_2) = |\mathbf{r}_1 - \mathbf{r}_2|^{-1}$  is the bare Coulomb potential while  $w(\mathbf{r}_1, \mathbf{r}_2) = \int \varepsilon^{-1}(\mathbf{r}_1, \mathbf{r}) v(\mathbf{r}, \mathbf{r}_2) d\mathbf{r}$  is the screened one. The excitonic eigenenergies  $E_x$  and eigenstates  $\mathbf{A}$  are provided by the solution of the above eigenvalue problem; hence, this description [20] closely resembles the earlier one obtained within a Green's function scheme, which comprises the solution of the Bethe-Salpeter equation [21, 22].

The first step is therefore the calculation of non-interacting electron and hole quasiparticle energies  $\bar{\epsilon}$  and wavefunctions  $\psi$  that we obtain through a density-functional theory hamiltonian in the local density approximation [23, 24] (with norm-conserving pseudopotentials and a plane-wave basis with 50 Ry energy cutoff), and by subsequently adding a rigid shift to the conduction band energies to account for the self-energy correction (taken from Ref. 2). Moreover, in order to make the full calculation computationally feasible for complex systems as polymer crystals, we approximate the full effective screening function by a constant diagonal dielectric tensor  $\underline{\underline{\varepsilon}}$ , whose components are calculated *ab initio* within linear response [24]. For the case of the isolated polymer chain, the assumption of space homogeneity is indeed very drastic, so we introduce an effective screening tensor, which is defined within the volume  $\Omega_{\text{eff}}$  where the interaction actually takes place, while  $\underline{\underline{\varepsilon}} = 1$  outside  $\Omega_{\text{eff}}$ . The components of  $\underline{\underline{\varepsilon}}$  are again calculated *ab initio* within linear response and  $\Omega_{\text{eff}}$  is determined self-consistently with  $\underline{\underline{\varepsilon}}$  to encompass the region of significant electron-hole correlation function.

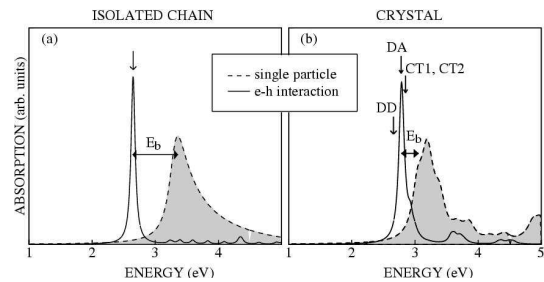


FIG. 1:  $z$ -polarized optical spectra for single chain PPV (left) and the PPV crystal in herring-bone structure (right). The solid lines are the  $z$ -polarized spectra calculated including electron-hole Coulomb interaction; the single particle spectra are shown for comparison as shaded backgrounds. An artificial broadening of 0.04 eV (0.08 eV) was included for plotting the Coulomb-correlated (single particle) spectra. The exciton binding energy is the energy difference between the exciton absorption peak in the correlated spectrum and the onset of the continuum in the single-particle spectrum. The arrows mark the lowest singlet exciton in the isolated chain spectrum, and relevant singlet excited states in the crystal spectrum: first optically active direct exciton (DA), optically inactive (dark) direct exciton (DD); charge-transfer excitons (CT1 and CT2).

In order to better understand the role of interchain coupling for the crystal case, we first consider the isolated chain as reference system. We show in Fig. 1(a) the results for the absorption spectrum of the isolated chain [2, 3], which is highly polarized along the chain ( $z$ -direction); for  $x$  and  $y$  polarizations absorption close to band gap is negligible. We find an optically active  $^1B_u$  singlet exciton with energy approximately 0.6–0.7 eV below the single-particle band-gap energy. This lowest singlet state extends over a few unit cells along the chain [2, 3], the large binding energy arising essentially from the strong lateral confinement. To gain insight in the nature of this state, in Fig. 2 we plot its electron and hole contributions:  $\rho^h(\mathbf{r}_h) = \sum_\mu |\sum_\nu A_{\mu\nu} \psi_\nu^h(\mathbf{r}_h)|^2$  and  $\rho^e(\mathbf{r}_e) = \sum_\nu |\sum_\mu A_{\mu\nu} \psi_\mu^e(\mathbf{r}_e)|^2$ . Both have their maxima on the vinylene chains but in different bonding configurations, and thus vinylene atoms are expected to undergo the largest photoinduced lattice relaxation; this suggests the assignment of the phonon replica observed in PPV photoluminescence to the vinylene C-C stretch mode (around 0.2 eV [25, 26, 27, 28]) and explains the difference in lineshape [29] with poly-*para*-phenylene (PPP), where the vinylene chains are not present.

We point out that the exciton signature is accompanied by suppression of the typical 1D van Hove singularity ( $\sim 1/\sqrt{E}$ ) [3]. This is a phenomenon resulting from dimensionality, also found in inorganic semiconductor quantum wires [18, 30]. It is relevant for the experimental determination of the exciton binding energy: the energy separation between the exciton and the onset of the 1D absorption continuum cannot be extracted

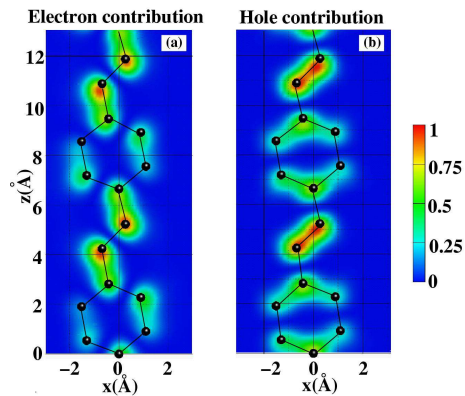


FIG. 2: Electron and hole contributions,  $\rho^e$  (a) and  $\rho^h$  (b), to the lowest singlet exciton of the isolated PPV chain, plotted in a plane parallel to the phenyl rings. The colour code is shown on the side bar, with  $\rho^e$  ( $\rho^h$ ) normalized to its maximum value.

directly from a one-photon optical spectrum, since the oscillator strength associated to the latter is vanishingly small [18]; a separate measurement is required to extract the quasiparticle gap [5, 7, 8, 31].

We now turn to the PPV crystal, that we calculate in a realistic herring-bone structure [32, 33], by keeping an orthorhombic cell with  $a = 8.07$  Å,  $b = 5.08$  Å,  $c = 6.54$  Å and the setting angle  $\Phi = 52^\circ$  (see inset in Fig. 3). The influence of crystalline structure can be felt already on the single-particle bands: due to the specific crystal symmetry, with two chains per unit cell, all bands are doubled [33]; the splitting between doublets gives rise to the splitting between excitonic states (the so-called Davydov splitting [34]), and is strongly dependent on interchain interaction. This feature alone points to a clear difference between PPV and other substituted PPV derivatives, such as MEH-PPV, that cannot pack in the herring-bone structure, have only one chain per cell, and thus would not show Davydov splittings. Note that this very important feature cannot be seen either from structureless crystal models [4] or simple molecular aggregate models without translational symmetry [35]. Other general features are that dispersion along the  $\Gamma$ -Z direction (along the chain) is of the order of  $\sim 2.2$  eV, as for the isolated chain, and dispersion perpendicular to the chain is vanishingly small.

We show in Fig. 1(b) the correlated spectrum for the crystal. It is again characterized by a strong singlet exciton peak (marked DA in the figure) and quenching of the oscillator strength at the onset of the single-particle continuum. While the single-particle band gap is reduced in the crystal [33], the optical gap in the correlated spectrum is close to the single-chain result. Hence, the binding energy of this exciton is reduced to about 0.2 eV, consistent with the increased screening in the crystal [4]. The first absorption peak is still strongly polarized along

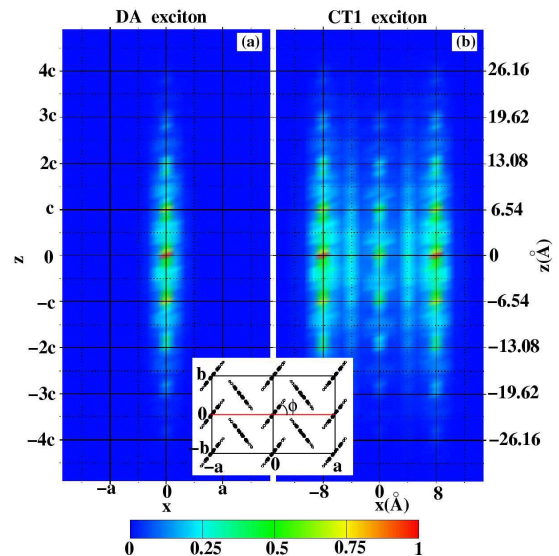


FIG. 3: Probability distribution  $|\Psi^{exc}(\mathbf{r}_e, \mathbf{r}_h)|^2$  of the lowest singlet excitons in the PPV crystal. The state (a) is the optically active direct exciton DA appearing in the spectra of Fig. 1, while the state (b) corresponds to the dark state CT1, at slightly higher energy. Here  $\Psi^{exc}$  is plotted as a function of the electron-hole distance in the  $xz$  plane (red line in the inset) averaged over the center-of-mass coordinate  $\mathbf{R} = (\mathbf{r}_e + \mathbf{r}_h)/2$ . The colour code is shown below the figure, with the probability normalized to its maximum value in each panel. The inset shows a representation of the chains projection on the (a,b) plane of the orthorhombic cell.

$z$ , confirming the strong optical anisotropy of the material.

Now we turn our attention to the other remarkable features of the optical behavior: (a) the single-particle band-splitting results in an exciton Davydov splitting of  $\sim 120$  meV, with the corresponding introduction of an optically inactive (dark) state *below* the first active exciton (DD arrow in the figure); (b) other excitonic states are also introduced above the DA peak, with no oscillator strength along  $z$ , but just barely active on the perpendicular polarization (CT1 and CT2 in the figure).

The corresponding exciton wavefunctions for DA and CT1 are shown in Fig. 3, where we plot the probability density distributions  $|\Psi^{exc}(\mathbf{r}_e, \mathbf{r}_h)|^2$ . Note that the exciton wavefunction  $\Psi^{exc}(\mathbf{r}_e, \mathbf{r}_h)$ , expressing the probability amplitude of finding the electron in  $\mathbf{r}_e$  and the hole in  $\mathbf{r}_h$ , is computed within our formalism directly in terms of the interband polarization  $\mathbf{A}$  as  $\Psi^{exc}(\mathbf{r}_e, \mathbf{r}_h) = \sum_{\mu\nu} A_{\mu\nu} \psi_{\mu}^e(\mathbf{r}_e) \psi_{\nu}^{h*}(\mathbf{r}_h)$ . The DA state is remarkably confined on a single chain, only slightly more extended in  $z$ -direction than in the isolated chain. (The DD state has the same distribution as the DA, by symmetry: they are both direct as electrons and holes are on the same chain.) The CT1 state, on the other hand, shows very small on-chain contribution, with high probability of finding electron and hole on different chains, and can be character-

ized as an excimer; same comments apply to the CT2 state.

In summary, we have found that the lowest correlated states of PPV crystal do involve more than one chain and are very dependent on crystal structure [16]; however, they retain a quasi-one-dimensional character, and the consequent suppression of 1D singularity precludes the use of one-photon experiments to extract exciton binding energies. Furthermore, we have found that, due to interchain coupling and symmetry effects, the lowest electronic excitation is a dark exciton, that is optically inactive but provides a non-radiative decay path. This can strongly quench the photoluminescence with respect to non-interacting chains. In view of the impact of crystallization on the optical properties, we studied also the influence of the packing density: without changing the symmetry, we increased the interchain distance in the  $\pi$ -stack direction  $b$  (see inset in Fig. 3); we find that an increase of  $\simeq 20\%$  leads to an increase in the binding energy (to  $\simeq 0.4$  eV) and a drastic decrease in the Davydov splitting by an order of magnitude, thus restoring radiative efficiency. These results suggest that the spread in photoluminescence (PL) and photoconductivity (PC) data observed by different groups may arise from differences in the aggregation state of the polymer. Moreover, since real films have regions with different chain packings, the dominant contributions to PL and PC can originate from different regions of the same sample (the least and the most closely packed, respectively). Another solid state effect is the appearance of bound charge-transfer excitations close above the first exciton peak: this not only can enhance photoconductivity, but also can be the origin of the infra-red active modes seen on two-photon experiments [10, 36].

Our results show that solid state effects are indeed very important for the final optical structure of a polymer film. This conclusion could only be reached because of the possibility of calculating first-principles optical spectra of realistic three-dimensional polymer structures.

We are grateful to Fausto Rossi for many relevant suggestions in the early stages of this work. We also thank Ulrich Hohenester, Lucia Reining, Eric K. Chang, and Guido Goldoni for useful discussion. This work was supported in part by MURST (Cofin-99) - Italy, by FAPESP - Brazil, and by a CNR-CNPq bilateral project.

---

[1] R. H. Friend et al., *Nature* **397**, 121 (1999).

[2] M. Rohlfling and S. G. Louie, *Phys. Rev. Lett.* **82**, 1959 (1999).

[3] A. Ruini et al., *Synth. Met.* **119**, 257 (2001).

- [4] J. W. van der Horst, P. A. Bobbert, M. A. J. Michels, G. Brocks, and P. J. Kelly, *Phys. Rev. Lett.* **83**, 4413 (1999).
- [5] M. G. Leng et al., *Phys. Rev. Lett.* **72**, 156 (1994).
- [6] M. Chandross et al., *Phys. Rev. B* **55**, 1486 (1997).
- [7] S. F. Alvarado, P. F. Seidler, D. G. Lidsey and D. D. C. Bradley, *Phys. Rev. Lett.* **53**, 16462 (1996); L. Rossi et al. *Synth. Met.* **334**, 303 (2001).
- [8] I. H. Campbell, T. W. Hagler, D. L. Smith, and J. P. Ferraris, *Phys. Rev. Lett.* **76**, 1900 (1996).
- [9] S. Barth and H. Bässler, *Phys. Rev. Lett.* **79**, 4445 (1997).
- [10] D. Moses, J. Wang, A. J. Heeger, N. Kirova, and S. Brazovskii, *Synth. Met.* **125**, 93 (2001).
- [11] E. M. Conwell, *Synth. Met.* **83**, 101 (1996).
- [12] M. W. Wu and E. M. Conwell, *Phys. Rev. B (RC)* **56**, R10060 (1997).
- [13] M. Yan, L. J. Rothberg, E. W. Kwock, and T. M. Miller, *Phys. Rev. Lett.* **75**, 1992 (1995).
- [14] S. V. Frolov, Z. Bao, M. Wohlgenannt, and Z. V. Vardeny, *Phys. Rev. Lett.* **85**, 2196 (2000).
- [15] M. Muccini et al., *Phys. Rev. B* **62**, 6296 (2000).
- [16] G. Bussi et al., to be published (2002).
- [17] I. G. Hill, A. Kahn, Z. S. Soos, and R. A. Pascal, *Chem. Phys. Lett.* **327**, 181 (2000).
- [18] F. Rossi and E. Molinari, *Phys. Rev. Lett.* **76**, 3642 (1996); *Phys. Rev. B* **53**, 16462 (1996).
- [19] D. Beljonne, Z. Shuai, J. Cornil, D. A. dos Santos, and J. L. Brédas, *J. Chem. Phys.* **111**, 2829 (1999).
- [20] U. Hohenester, *Phys. Rev. B* **64**, 205305 (2001).
- [21] L. J. Sham and T. M. Rice, *Phys. Rev.* **144**, 708 (1966).
- [22] W. Hanke and L. J. Sham, *Phys. Rev. Lett.* **43**, 387 (1979).
- [23] W. Kohn and L. J. Sham, *Phys. Rev.* **140**, A1133 (1965).
- [24] S. Baroni, A. D. Corso, S. de Gironcoli, and P. Giannozzi, 2001, <http://www.pwscf.org>.
- [25] B. Tian, G. Zerbi, and K. Müllen, *J. Chem. Phys.* **95**, 3198 (1991).
- [26] A. Sakamoto, Y. Furukawa, and M. Tatsumi, *J. Phys. Chem.* **96**, 1490 (1992).
- [27] S. J. Martin, D. D. C. Bradley, P. A. Lane, H. Mellor, and P. L. Burn, *Phys. Rev. B* **59**, 15133 (1999).
- [28] R. B. Capaz and M. J. Caldas, to be published (2002).
- [29] H. Eckhardt, L. W. Shacklette, K. Y. Jen, and R. L. Elsenbaumer, *J. Chem. Phys.* **91**, 1303 (1989).
- [30] T. Ogawa and T. Takagahara, *Phys. Rev. B* **44**, 8138 (1991).
- [31] R. Rinaldi et al., *Phys. Rev. B* **63**, 075311 (2001).
- [32] D. Chen, M. J. Winokur, M. A. Masse, and F. E. Karasz, *Polymer* **33**, 3116 (1992).
- [33] P. Gomes da Costa and E. M. Conwell, *Phys. Rev. B* **48**, R1993 (1993).
- [34] A. S. Davydov, *Theory of Molecular Excitons*, McGraw-Hill, 1962.
- [35] J. Cornil, J. P. Calbert, D. Beljonne, R. Silbey, and J. L. Brédas, *Synth. Met.* **119**, 1 (2001).
- [36] D. Moses, A. Dogariu, and A. J. Heeger, *Chem. Phys. Lett.* **316**, 356 (2000).